Materials for Quantum Technology

PAPER

Design and validation of a-SiC/SiN hybrid photonic platform for integrated quantum photonics

Naresh Sharma[1,3,*], Zizheng Li[1,3], Bruno Lopez-Rodriguez[1,3], Joey Vrugt[1], Stijn van der Waal[1], Luozhen Li[1], Roald van der Kolk[1], Philip J Poole[2], Dan Dalacu[2] and Iman Esmaeil Zadeh[1]

[1] Department of Imaging Physics (ImPhys), Faculty of Applied Sciences, Delft University of Technology, Delft 2628 CJ, The Netherlands
[2] National Research Council Canada, Ottawa, ON, Canada
[3] The authors contributed equally to this work.
[*] Author to whom any correspondence should be addressed.

E-mail: N.Sharma-1@tudelft.nl

Keywords: quantum dots, single photon, quantum photonic integrated circuits, superconducting nanowire single photon detectors, silicon carbide

OPEN ACCESS

RECEIVED
16 April 2024

REVISED
28 June 2024

ACCEPTED FOR PUBLICATION
17 September 2024

PUBLISHED
26 September 2024

Abstract

Recent efforts in quantum photonics emphasize on-chip generation, manipulation, and detection of single photons for quantum computing and quantum communication. In quantum photonic chips, single photons are often generated using parametric down-conversion and quantum dots. Quantum dots are particularly attractive due to their on-demand generation of high-purity single photons. Different photonic platforms are used to manipulate the states of the photons. Nevertheless, no single platform satisfies all the requirements of quantum photonics, as each platform has its merits and shortcomings. For example, the thin-film silicon nitride (SiN) platform provides ultra-low loss on the order of 0.1 dB m^{-1}, but is incompatible with dense integration , requiring large bending radii. On the other hand, silicon on insulator offers a high refractive index contrast for dense integration but has a high absorption coefficient at the emission wavelengths (800–970 nm) of state-of-the-art QDs. Amorphous silicon carbide (a-SiC) has emerged as an alternative with a high refractive index (higher than SiN), an extended transparency window compared to Silicon, and a thermo-optic coefficient three times higher than that of SiN, which is crucial for tuning photonic devices on a chip. With the vision of realizing a quantum photonic integrated circuit, we explore the hybrid integration of SiN/a-SiC photonic platform with quantum dots and superconducting nanowire single-photon detectors. We validate our hybrid platform using a brief literature study, proof-of-principle experiments, and complementary simulations. As a proof-of-principle, we show a quantum dot embedded in nanowires (for deterministic micro-transfer and better integration) that emits single photons at 885 nm with a purity of 0.011 and a lifetime of 0.98 ns. Furthermore, we design and simulate an adiabatic coupler between two photonic platforms, a-SiC and SiN, by aiming to use the benefits of both platforms, i.e. dense integration and low losses, respectively. Our design couples the light from SiN waveguide to a-SiC waveguide with 96% efficiency at 885 nm wavelength. Our hybrid platform can be used to demonstrate on-chip quantum experiments such as Hong–Ou–Mandel, where we can design a large optical delay line in SiN and an interference circuit in a-SiC.

1. Introduction

In recent years, advancements in quantum technologies have harnessed the unique behavior of light particles, enhancing sensing, communication, and computing. Quantum sensors deliver unprecedented precision for measurements [1]. Quantum communication enables unhackable, long-distance data transmission [2]. Quantum computers promise exponential speedup for complex mathematical problems, while quantum cryptography ensures unbreakable data security [3]. Linear Optical Quantum Computers

(LOQC) use photons as quantum bits (qubits) and manipulate them using optical components such as mirrors, lenses, beam splitters, phase shifters, and detectors [4–7]. Although one can easily tweak discrete optical elements to fine-tune them for various requirements, such as low loss and high throughput, their bulky nature makes them impractical in terms of scalability. Therefore, quantum photonic integrated circuits (QPIC) are essential to meet the growing demand for more sophisticated experiments [8]. Progress is being made to integrate all passive and active photonic devices, modulators, quantum frequency converters, high-performance detectors, and light sources on a single photonic platform [9–16]. In addition, many groups are exploring and characterizing different photonic platforms that satisfy all the requirements for efficient quantum photonic integrated circuits, i.e. low photonic loss, high integration density, large tuning range, optical non-linearities, and CMOS compatibility [17–20]. However, thus far, no single material platform offers all the mentioned requirements. One of the effective ways to address the need for quantum photonic integrated circuits is hybrid integration that connects various devices composed of different materials on a single chip at the fabrication level. The main challenges in hybrid integration are compatibility issues, yield, and efficient coupling between various optical devices fabricated in different layers and materials. This work proposes a method to combine two promising photonic platforms, i.e. a-SiC and SiN, and integrate them with III–V sources and superconducting detectors on the same chip. We design and simulate an adiabatic coupler to couple the light from thin-film SiN to a-SiC with 96% efficiency. This configuration (i.e. SiC/SiN) offers the advantages of both SiN (low-loss) and a-SiC (dense integration). We also characterize the InAsP/InP quantum dots embedded in InP nanowires as a single-photon source. We generate single photons with high purity and short lifetime and, through literature review, illustrate our vision of their future integration with photonic circuits and single photon detectors.

2. Generation of single-photons

Many quantum photonic protocols demand on-chip single photon generation. In sources based on optical non-linearities, such as Spontaneous Parametric Down Conversion (SPDC) and Spontaneous Four Wave Mixing (SFWM), due to the probabilistic nature of the emission, deterministic generation of single photons is challenging [22, 23]. Moreover, strong pump fields are required to generate correlated photons through nonlinear effects, which makes the integration of sources and detectors impractical (challenging to distillate—e.g. filter- single photons in the presence of strong pump fields). On the other hand, quantum dots offer deterministic single-photon generation with high efficiency and precise and narrow emission bandwidth [24–31]. Also, QDs integration with photonic circuits has achieved great progress [32–39]. In recent years, the main challenge with QDs, i.e. photon indistinguishably, has also been addressed [40]. We investigate the potential of integrating nanowire quantum dots in hybrid photonic circuits. Figure 1(a) shows an illustrative image of a standing as-grown indium phosphide (InP) nanowire on a InP substrate with a length of 1.5–3 μm and diameter 250–300 nm. A 3–4 nm section of indium arsenide phosphide (InAsP) is grown in the nanowire at 200 nm from the base to create the quantum dot [24]. To characterize and select an emitter with the desired characteristics to transfer to the photonic chips, we place the sample in a Helium flow cryostat with a base temperature $<$6 K. Figure 1(b) represents the schematic of our experimental setup. We locate quantum dots by illuminating the sample surface using a light-emitting diode followed by an objective lens, and the reflection is collected in a camera (figure 1(b)). Afterward, we obtain the photoluminescence spectrum by exciting them with a continuous wave laser at a wavelength of 785 nm (non-resonant excitation). The emitted photons are collected using the same optical path in the reflection geometry. The excitation wavelength is blocked with a long pass filter (Thorlabs LP850). Figure 1(c) shows the emission spectrum of a quantum dot measured using a spectrometer (monochromator Acton series SP-2750 from Princeton Instruments) with 1800 grooves per millimeter grating. We fit this narrowband spectrum with a Lorentzian function (inset of figure 1(c)) and determine the emission wavelength as 884.8 nm, the emission linewidth is less than the resolution limit of our spectrometer (spectrometer resolution ~30–45 pm). High resolution measurements using an etalon on similar nanowire quantum dots indicates linewidths less than 1.1 pm [41]. Single photon purity and indistinguishability are critical for the operation of quantum technologies, including quantum computing and quantum communication. To determine the single photon purity of the nanowire quantum dots, we perform a fiber-based Hanbury Brown and Twiss experiment and calculate the second-order correlation $g^{(2)}$ (figure 1(d)). We detect these single photons using a self-aligned fiber-coupled superconducting nanowire single-photon detector (SNSPD). The emitted light from the quantum dots is coupled from the spectrometer to a paddle polarization controller and a polarization maintaining fiber-coupled beamsplitter (PBC980PM-FC). The polarization going to the SNSPDs is aligned to the TE mode of the SNSPDs corresponding to the highest system detection efficiency. A time-tagger is used to determine the time of arrival of the photons in the two detectors and build a correlation histogram. The measured multiphoton emission probability $g^{(2)}(0)$, calculated by fitting the experimental data (red

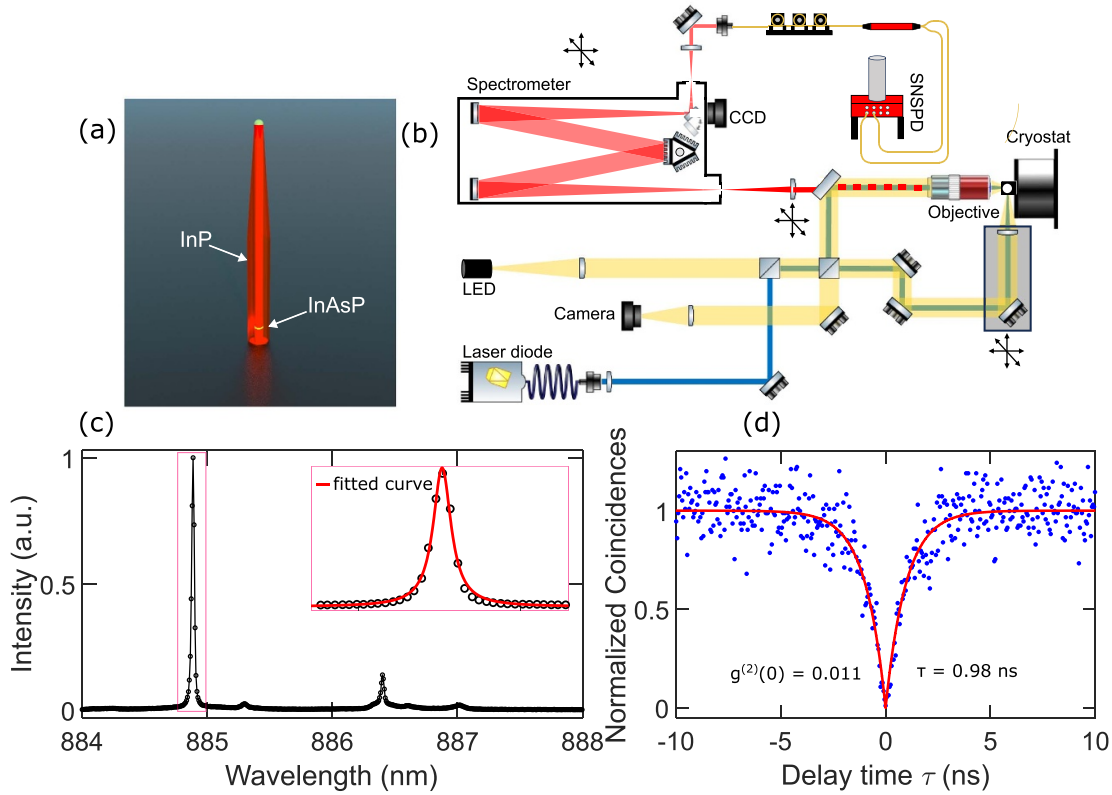

Figure 1. (a) An illustration [21] of a nanowire quantum dot, similar to those used in this study. (b) Schematic of the optical setup used to characterize quantum dots. The setup allows for both top and side access; in this study only top access was used. (c) Measured emission spectrum of a quantum dot. The emission wavelength is 884.8 nm. (d) Second-order correlation measurement ($g^{(2)}$) showing multiphoton emission probability as low as 0.011. The lifetime of the quantum dots is 0.98 ns.

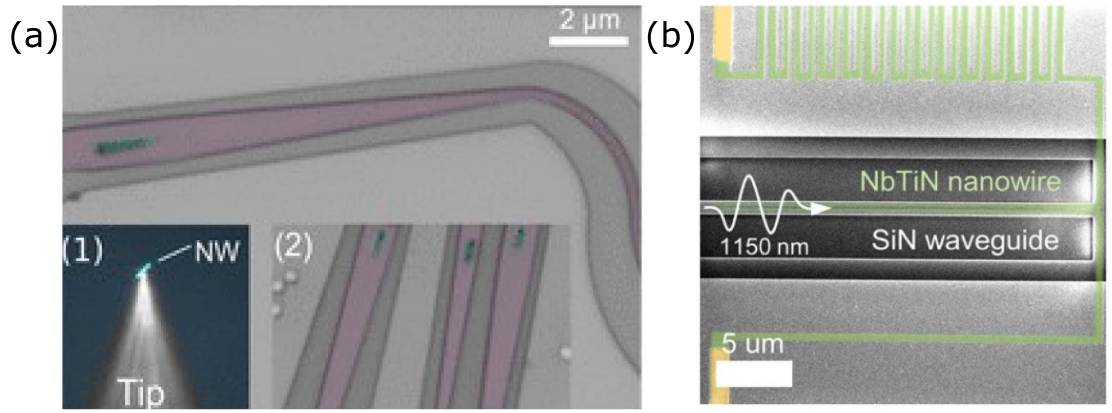

Figure 2. (a) Scanning electron microscope image of a nanowire quantum dots embedded in silicon nitride (SiN) waveguides. Reprinted (adapted) with permission from [33]. Copyright (2016) American Chemical Society. (b) Scanning electron microscope image of a silicon nitride (SiN) waveguide coupled to a superconducting nanowire single-photon detector (SNSPD) on a chip. Reprinted (adapted) with permission from [44]. Copyright (2019) American Chemical Society.

curve in figure 1(d)), is 0.011. Furthermore, we estimate an emission lifetime of the QDs as 0.98 ± 0.1 ns from the fitting curve (red curve in figure 1(d)). Reimer *et al* [42] (for as-grown nanowire quantum dots) and Yeung *et al* [43] (for a nanowire in a PIC) performed Hong–Ou–Mandel (HOM) (two-photon interference) experiment on similar nanowire quantum dots, and confirmed that the generated photons by nanowire QDs show a relatively high level of indistinguishably. This property reveals that the nanowire QDs generate identical photons with precisely the same properties, such as frequency, polarization, and spatial mode, and hence meet the requirements for the applications requiring photon interference.

Further, these QDs can be transferred on a photonic platform without affecting their emission quality [33]. Figure 2(a) shows the QDs embedded in the silicon nitride waveguides [33]. The QDs are first

transferred on a silicon substrate using a nanomanipulator (pick-and-place method). Afterward, a silicon nitride film is deposited and patterned to define the waveguides. Similarly, the detectors can also be integrated with the waveguide on a chip. Figure 2(b) shows an SNSPD encapsulated by a silicon nitride waveguide [44]. Advancements have been achieved in integrating quantum dots (QDs) and SNSPDs on the same chip to demonstrate basic quantum experiments. Schwartz *et al* [45]. demonstrated the on-chip single-photon Hanbury-Brown and Twiss Experiment by integrating the QDs and SNSPDs with a single-mode GaAs ridge waveguide. Nevertheless, the high waveguide losses of the photonic platform pose a primary impediment to the evolution of complex quantum photonic integrated circuits.

3. Hybrid integration of a-SiC and SiN

Different materials such as silicon nitride (SiN) [46, 47], silicon (Si) [48–50], lithium niobate (LN) [51–53], gallium arsenide (GaAs) [54, 55], indium phosphide (InP) [55–57], and silicon carbide (SiC) [15, 16, 58–66] have been used to demonstrate various on-chip photonic applications including switching, filtering, splitting, combining, amplification, modulation and many more. However, no single material meets all the requirements of an efficient and high-throughput photonic integrated circuit [67, 68]. For example, SiN waveguide deposited by low pressure chemical vapor deposition (LPCVD) with specific design parameters (thickness 40 nm and width 2 um) provides ultra-low losses of down to 0.1 dB m^{-1} (figure 3(a)) [32, 69]. This platform can be used for optical delay lines in quantum experiments such as HOM. However, these ultrathin film SiN waveguides are not scalable for applications that require strong confinement, such as integration of many modulators, phase shifters, filters, beam splitters, and other circuit components [70] as the bending losses, prohibits the require dense integration. The minimum bending radius in, for example, figure 3(a) is 1 mm. We adopt the same waveguide parameters and simulate the bending waveguides using FDTD simulation to characterize bending losses. The simulation wavelength was 885 nm, i.e. our quantum dot emission wavelength. Figure 3(b) shows the loss as a function of bending radius. Significant losses can be observed for bending radii below 400 μm, as the light is no longer confined in the waveguide. To avoid this problem, we propose hybrid integration of these ultra-low loss thin SiN films with other materials with high refractive index and
thickness.

Amorphous silicon carbide is a suitable material to be integrated with SiN due to its unique properties, such as high refractive index and a wide transparency window from the visible to the mid-infrared range. The refractive index of the a-SiC is higher than that of SiN [19]. In addition, the thermo optic coefficient of a-SiC is three times higher than SiN [63]. The thermo-optic coefficient is crucial for tuning the on-chip photonic devices; a high thermo-optic coefficient results in an extensive tuning range and reduces the thermal crosstalk between devices and quantum dots. The QDs embedded in the SiC waveguide provide unidirectional coupling efficiency greater than 86% [33].

Furthermore, the high-quality amorphous silicon carbide films can be deposited on wet thermal oxide on silicon substrate at low temperatures. Our recent work [63] presents a novel technique for low-temperature deposition of a-SiC thin films using Inductively Coupled Plasma Chemical Vapor Deposition (ICPCVD). With optimized deposition recipe (Temperature: 150 °C, Pressure: 2 mTorr, and ICP Power: 750 W), we deposit a-SiC films with surface roughness $<$1 nm and a deposition rate of 36 nm min^{-1}. Thanks to the low-temperature deposition (half the temperature than in standard PECVD process), our method is compatible with standard lift-off techniques, allowing monolithically integrating devices with different thickness without interfering other photonic components on the same chip. Using this lift-off scheme, we deposited the a-SiC films (figure 4(a)) and fabricated photonic components (figure 4(b)). In addition, we measured the optical properties of the a-SiC and SiN (figure 4(c)) using ellipsometry. Further, we show the fabrication flow to interface a-SiC film with SiN film (figure 4(d)). The fabrication starts from a stoichiometric SiN substrate where a layer of SiN is deposited by low-pressure chemical vapor deposition (LPCVD) on a wet oxidized silicon wafer. Electron-beam lithography (EBL) and reactive ion etching (RIE) are then performed to define the photonic integrated circuits on the SiN layer. A thin layer of ICPCVD silicon dioxide (SiO_2) is put on top as a spacer, preventing any possible damage to the SiN layer in the subsequent processes. After which, we use low-temperature ICPCVD and standard lift-off processes to deposit the a-SiC layer and define the devices. Finally, polymethyl methacrylate (PMMA) is coated over the sample as optical cladding.

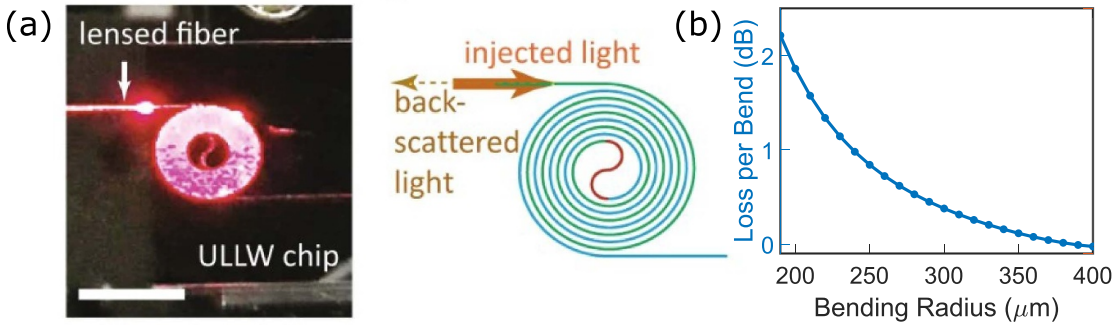

Figure 3. (a) Optical microscope image and schematic of an ultra-low loss waveguide spiral with 1 m length. Reproduced from [32]. CC BY 4.0. (b) Simulated loss, for similar waveguides as shown in part (a), as a function of bending radius.

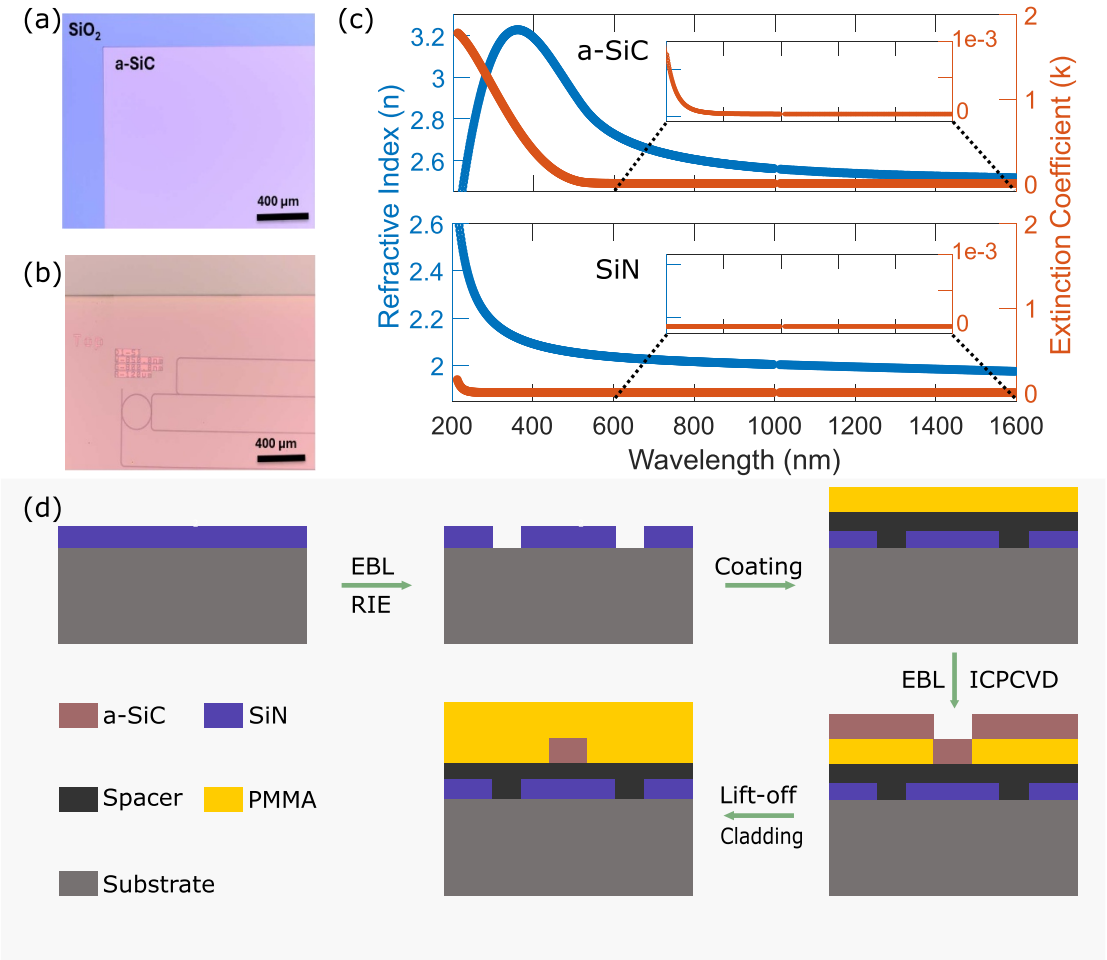

Figure 4. (a) Optical image of a-SiC film deposited using lift-off method at a temperature of 150 °C. (b) Optical image of a ring-resonator fabricated on the a-SiC film. (c) Measured optical properties of the SiN and a-SiC films using ellipsometry. (d) Fabrication flow to interface a-SiC film to SiN film..

4. Design of an adiabatic coupler

Despite the unique properties of SiN and SiC, the real challenge is to efficiently couple the light interchangeably from one material to another in a hybrid configuration. We take this challenge and design an adiabatic coupler between the waveguides of these two materials (i.e. SiN and SiC). For efficient coupling from the SiN waveguide to the SiC waveguide, the effective refractive index and mode profile of both the waveguides should perfectly match. We calculate the effective refractive index of both waveguides for fundamental TE mode as a function of waveguide width (figure 5(a)). As one decreases the waveguide

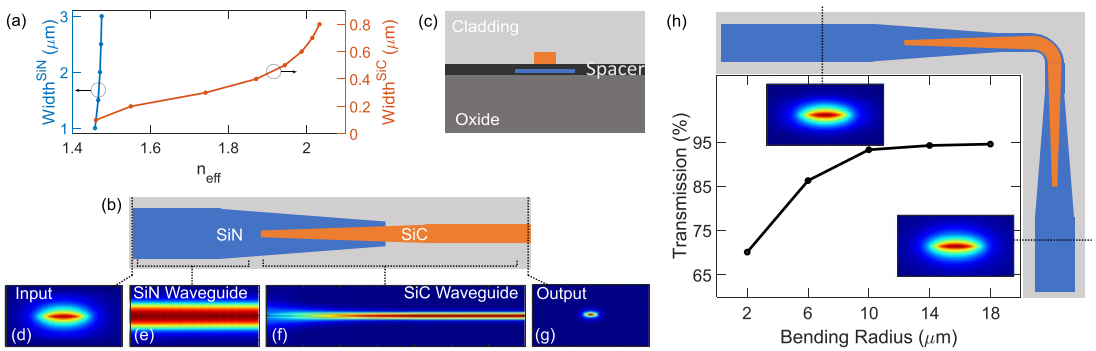

Figure 5. (a) The effective refractive index of the SiN (solid blue) and SiC (solid brown) waveguides as a function of their width. (b) Planer and (c) cross-sectional view of the adiabatic coupler. (d) Cross-sectional intensity distribution in SiN waveguide. Planar intensity distribution in (e) SiN and (f) SiC waveguide. (g) Cross-sectional intensity distribution in SiC waveguide. (h) Designed structure to achieve low-loss and sharp bends in low-loss SiN platform, using a SiC section.

widths, the effective refractive index of the waveguides decreases, and in both cases (1 um wide, 40 nm thick SiN waveguide and 100 nm wide, 100 nm thick SiC waveguide), it reaches the same effective refractive index (1.46) (figure 5(a)). Considering the relation between width and the effective refractive index, we design our adiabatic coupler by tapering the SiN width from 2 um to 1 um and SiC width from 400 nm to 100 nm (figure 5(b)). The figure 5(c) shows the cross-section view of our designed coupler. The SiC waveguide is placed on top of the SiN waveguide with a spacer layer of 20 nm (SiO_2) and covered with a thick oxide (SiO_2) layer as cladding (figure 5(c)). We simulate (FDTD) the designed adiabatic coupler by exciting the fundamental TE mode (figure 5(d)) of the SiN waveguide. Figures 5(e) and (f) show the normalized field distribution in the SiN waveguide (before the coupling) and in the a-SiC waveguide (after the coupling), respectively. Our coupler couples most of the light from SiN waveguide to a-SiC waveguide with an efficiency of 96%. Figure 5(g) shows the output mode profile (cross-section) of the a-SiC waveguide after the coupling.

We use this adiabatic coupler to bend the low-loss SiN waveguide of different radii and calculate the transmissions (figure 5(h)). The light first travels in the SiN waveguide and couples to the SiC waveguide in the bending region, and then it is coupled back to the SiN waveguide. This configuration guides the light with an in-out efficiency of 94% for bending radius 14 μm. The inset of figure 5(h) shows the mode profile of the SiN waveguide before and after the bending. The designed adiabatic coupler acts like a bridge for hybrid integration of two promising material platforms of thin-film SiN and a-SiC.

5. Conclusion and discussion

In conclusion, we have characterized InAsP/InP nanowire quantum dots by measuring the photolumines–cence and second-order correlation in a cryostat. Our quantum dots generate single photons with high purity of ~1%. We discussed the prospect of integrating our nanowire quantum dots and superconducting nanowire single photon detectors into photonic platforms. Additionally, we have designed and simulated an adiabatic coupler for hybrid integration of SiN and a-SiC photonic platforms. The adiabatic coupler couples light from the SiN waveguide to the a-SiC waveguide with an efficiency of 96% in simulation. As a proof-of-principle, we have shown that the adiabatic coupler overcomes the bending losses in thin film SiN waveguide by coupling the light in/out to/from a-SiC waveguide within the bending region. This configuration uses both the strengths of a high-index and high scalability platform (e.g. SiC) and a low-index and low loss mediums (e.g. SiN) deposited on the same chip. The full envisioned platform includes QDs, SNSPds, low loss delay lines (on SiN), and photonic circuits e.g. beamsplitters, phase shifters etc (on SiC) on the same chip. Integrating all the required elements of quantum photonics on a single chip can open way for the efficient and scalable implementation of sophisticated quantum experiments.

Data availability statement

All data that support the findings of this study are included within the article (and any supplementary files).

Conflict of interest

The authors declare no other competing interest.

Funding sources

N S acknowledges the NWO OTP COMB-O Project (18757). Z L acknowledges the China Scholarship Council (CSC, 202206460012). I E Z acknowledge funding from the European Union's Horizon Europe research and innovation programme under Grant Agreement No. 101098717 (RESPITE project) and Number 101099291 (fastMOT project).

Disclosures

I E Z has a part-time appointment at Single Quantum B.V., Rotterdamseweg 394, 2629 HH, Delft, The Netherlands.

ORCID iDs

Naresh Sharma https://orcid.org/0009-0005-6489-8512
Zizheng Li https://orcid.org/0000-0001-8139-8660
Stijn van der Waal https://orcid.org/0009-0007-8663-730X
Luozhen Li https://orcid.org/0009-0006-2265-3418
Dan Dalacu https://orcid.org/0000-0001-6204-3952
Iman Esmaeil Zadeh https://orcid.org/0000-0002-3833-2508

References

[1] Pirandola S, Bardhan B R, Gehring T, Weedbrook C and Lloyd S 2018 Advances in photonic quantum sensing *Nat. Photon.* **12** 724–33
[2] Chen Y-A *et al* 2021 An integrated space-to-ground quantum communication network over 4,600 kilometres *Nature* **589** 214–9
[3] Portmann C and Renner R 2022 Security in quantum cryptography *Rev. Mod. Phys.* **94** 025008
[4] Knill E, Laflamme R and Milburn G J 2001 A scheme for efficient quantum computation with linear optics *Nature* **409** 46–52
[5] Kok P, Munro W J, Nemoto K, Ralph T C, Dowling J P and Milburn G J 2007 Linear optical quantum computing with photonic qubits *Rev. Mod. Phys.* **79** 135
[6] Wang H *et al* 2019 Boson sampling with 20 input photons and a 60-mode interferometer in a 10^{14}-dimensional Hilbert space *Phys. Rev. Lett.* **123** 250503
[7] Deng Y-H *et al* 2023 Gaussian boson sampling with pseudo-photon-number-resolving detectors and quantum computational advantage *Phys. Rev. Lett.* **131** 150601
[8] Pelucchi E *et al* 2022 The potential and global outlook of integrated photonics for quantum technologies *Nat. Rev. Phys.* **4** 194–208
[9] Yan J, Fang L, Sun Z, Zhang H, Yuan J, Jiang Y and Wang Y 2023 Complete active–passive photonic integration based on GaN-on-silicon platform *Adv. Photon. Nexus* **2** 046003–046003
[10] Pohl D *et al* 2020 An integrated broadband spectrometer on thin-film lithium niobate *Nat. Photon.* **14** 24–29
[11] Wang X, Jiao X, Wang B, Liu Y, Xie X-P, Zheng M-Y, Zhang Q and Pan J-W 2023 Quantum frequency conversion and single-photon detection with lithium niobate nanophotonic chips *npj Quantum Inf.* **9** 38
[12] Patel R N, Schröder T, Wan N, Li L, Mouradian S L, Chen E H and Englund D R 2016 Efficient photon coupling from a diamond nitrogen vacancy center by integration with silica fiber *Light Sci. Appl.* **5** e16032
[13] McKenna T P, Stokowski H S, Ansari V, Mishra J, Jankowski M, Sarabalis C J, Herrmann J F, Langrock C, Fejer M M and Safavi-Naeini A H 2022 Ultra-low-power second-order nonlinear optics on a chip *Nat. Commun.* **13** 4532
[14] Peralta Amores A and Swillo M 2022 Low-temperature bonding of nanolayered InGaP/SiO_2 waveguides for spontaneous-parametric down conversion *ACS Appl. Nano Mater.* **5** 2550–7
[15] Zhu Y *et al* 2022 Hybrid integration of deterministic quantum dot-based single-photon sources with CMOS-compatible silicon carbide photonics *Laser Photonics Rev.* **16** 2200172
[16] Si M, Zhou L, Peng W, Zhang X, Yi A, Wang C, Zhou H, Wang Z, Ou X and You L 2023 Superconducting nanowire single photon detector on 4H-SiC substrates with saturated quantum efficiency *Appl. Phys. Lett.* **123** 131106
[17] Liu J, Huang G, Wang R N, He J, Raja A S, Liu T, Engelsen N J and Kippenberg T J 2021 High-yield, wafer-scale fabrication of ultralow-loss, dispersion-engineered silicon nitride photonic circuits *Nat. Commun.* **12** 2236
[18] Xing P, Ma D, Ooi K J A, Choi J W, Agarwal A M and Tan D 2019 CMOS-compatible PECVD silicon carbide platform for linear and nonlinear optics *ACS Photonics* **6** 1162–7
[19] Xing P, Ma D, Kimerling L C, Agarwal A M and Tan D T H 2020 High efficiency four wave mixing and optical bistability in amorphous silicon carbide ring resonators *APL Photonics* **5** 076110
[20] Stanfield P, Leenheer A, Michael C, Sims R and Eichenfield M 2019 CMOS-compatible, piezo-optomechanically tunable photonics for visible wavelengths and cryogenic temperatures *Opt. Express* **27** 28588–605
[21] Dalacu D, Poole P J and Williams R L 2021 Tailoring the geometry of bottom-up nanowires: application to high efficiency single photon sources *Nanomaterials* **11** 1201
[22] Xiong C, Bell B and Eggleton B J 2016 CMOS-compatible photonic devices for single-photon generation *Nanophotonics* **5** 427–39
[23] Liu F *et al* 2018 High Purcell factor generation of indistinguishable on-chip single photons *Nat. Nanotechnol.* **13** 835–40
[24] Dalacu D, Mnaymneh K, Lapointe J, Wu X, Poole P J, Bulgarini G, Zwiller V and Reimer M E 2012 Ultraclean emission from InAsP quantum dots in defect-free wurtzite InP nanowires *Nano Lett.* **12** 5919–23
[25] Versteegh M A M, Reimer M E, Jöns K D, Dalacu D, Poole P J, Gulinatti A, Giudice A and Zwiller V 2014 Observation of strongly entangled photon pairs from a nanowire quantum dot *Nat. Commun.* **5** 5298
[26] Reimer M E, Bulgarini G, Akopian N, Hocevar M, Bavinck M B, Verheijen M A, Bakkers E P A M, Kouwenhoven L P and Zwiller V 2012 Bright single-photon sources in bottom-up tailored nanowires *Nat. Commun.* **3** 737

[27] Mäntynen H, Anttu N, Sun Z and Lipsanen H 2019 Single-photon sources with quantum dots in III–V nanowires *Nanophotonics* **8** 747–69
[28] Bulgarini G, Reimer M E, Bouwes Bavinck M, Jöns K D, Dalacu D, Poole P J, Bakkers E P A M and Zwiller V 2014 Nanowire waveguides launching single photons in a Gaussian mode for ideal fiber coupling *Nano Lett.* **14** 4102–6
[29] Huang X, Horder J, Wong W W, Wang N, Bian Y, Yamamura K, Aharonovich I, Jagadish C and Tan H H 2024 Scalable bright and pure single photon sources by droplet epitaxy on InP nanowire arrays *ACS Nano* **18** 5581–9
[30] Zeuner K D *et al* 2021 On-demand generation of entangled photon pairs in the telecom C-band with InAs quantum dots *ACS Photonics* **8** 2337–44
[31] Becher C *et al* 2023 2023 roadmap for materials for quantum technologies *Mater. Quantum Technol.* **3** 012501
[32] Chanana A *et al* 2022 Ultra-low loss quantum photonic circuits integrated with single quantum emitters *Nat. Commun.* **13** 7693
[33] Zadeh I E, Elshaari A W, Jöns K D, Fognini A, Dalacu D, Poole P J, Reimer M E and Zwiller V 2016 Deterministic integration of single photon sources in silicon based photonic circuits *Nano Lett.* **16** 2289–94
[34] Elshaari A W, Zadeh I E, Fognini A, Reimer M E, Dalacu D, Poole P J, Zwiller V and Jöns K D 2017 On-chip single photon filtering and multiplexing in hybrid quantum photonic circuits *Nat. Commun.* **8** 379
[35] Davanco M, Liu J, Sapienza L, Zhang C-Z, De Miranda Cardoso J V, Verma V, Mirin R, Nam S W, Liu L and Srinivasan K 2017 Heterogeneous integration for on-chip quantum photonic circuits with single quantum dot devices *Nat. Commun.* **8** 889
[36] Uppu R *et al* 2020 On-chip deterministic operation of quantum dots in dual-mode waveguides for a plug-and-play single-photon source *Nat. Commun.* **11** 3782
[37] Kim J-H, Aghaeimeibodi S, Carolan J, Englund D and Waks E 2020 Hybrid integration methods for on-chip quantum photonics *Optica* **7** 291–308
[38] Li S *et al* 2023 Scalable deterministic integration of two quantum dots into an on-chip quantum circuit *ACS Photonics* **10** 2846–53
[39] Senellart P, Solomon G and White A 2017 High-performance semiconductor quantum-dot single-photon sources *Nat. Nanotechnol.* **12** 1026–39
[40] Zhai L, Nguyen G N, Spinnler C, Ritzmann J, Löbl M C, Wieck A D, Ludwig A, Javadi A and Warburton R J 2022 Quantum interference of identical photons from remote GaAs quantum dots *Nat. Nanotechnol.* **17** 829–33
[41] Laferrière P *et al* 2023 Approaching transform-limited photons from nanowire quantum dots using excitation above the band gap *Phys. Rev.* B **107** 155422
[42] Reimer M E *et al* 2016 Overcoming power broadening of the quantum dot emission in a pure wurtzite nanowire *Phys. Rev.* B **93** 195316
[43] Yeung E, Northeast D B, Jin J, Laferrière P, Korkusinski M, Poole P J, Williams R L and Dalacu D 2023 On-chip indistinguishable photons using III–V nanowire/SiN hybrid integration *Phys. Rev.* B **108** 195417
[44] Elsinger L *et al* 2019 Integration of colloidal PbS/CdS quantum dots with plasmonic antennas and superconducting detectors on a silicon nitride photonic platform *Nano Lett.* **19** 5452–8
[45] Schwartz M, Schmidt E, Rengstl U, Hornung F, Hepp S, Portalupi S L, Llin K, Jetter M, Siegel M and Michler P 2018 Fully on-chip single-photon Hanbury-Brown and Twiss experiment on a monolithic semiconductor–superconductor platform *Nano Lett.* **18** 6892–7
[46] Blumenthal D J, Heideman R, Geuzebroek D, Leinse A and Roeloffzen C 2018 Silicon nitride in silicon photonics *Proc. IEEE* **106** 2209–31
[47] Xiang C, Jin W and Bowers J E 2022 Silicon nitride passive and active photonic integrated circuits: trends and prospects *Photon. Res.* **10** A82–A96
[48] Heck M J R, Bauters J F, Davenport M L, Doylend J K, Jain S, Kurczveil G, Srinivasan S, Tang Y and Bowers J E 2012 Hybrid silicon photonic integrated circuit technology *IEEE J. Sel. Top. Quantum Electron.* **19** 6100117
[49] Dong P, Chen Y-K, Duan G-H and Neilson D T 2014 Silicon photonic devices and integrated circuits *Nanophotonics* **3** 215–28
[50] Siew S Y *et al* 2021 Review of silicon photonics technology and platform development *J. Lightwave Technol.* **39** 4374–89
[51] Chen G, Li N, Ng J D, Lin H-L, Zhou Y, Fu Y H, Lee L Y T, Yu Y, Liu A-Q and Danner A J 2022 Advances in lithium niobate photonics: development status and perspectives *Adv. Photonics* **4** 034003
[52] Boes A, Chang L, Langrock C, Yu M, Zhang M, Lin Q, Lončar M, Fejer M, Bowers J and Mitchell A 2023 Lithium niobate photonics: unlocking the electromagnetic spectrum *Science* **379** eabj4396
[53] Zhu D *et al* 2021 Integrated photonics on thin-film lithium niobate *Adv. Opt. Photonics* **13** 242–352
[54] Xie W, Xiang C, Chang L, Jin W, Peters J and Bowers J E 2022 Silicon-integrated nonlinear III–V photonics *Photon. Res.* **10** 535–41
[55] Roelkens G, Liu L, Liang D, Jones R, Fang A, Koch B and Bowers J 2010 III-V/silicon photonics for on-chip and intra-chip optical interconnects *Laser Photonics Rev.* **4** 751–79
[56] Yan Z, Han Y, Lin L, Xue Y, Ma C, Ng W K, Wong K S and Lau K M 2021 A monolithic InP/SOI platform for integrated photonics *Light Sci. Appl.* **10** 1–10
[57] Smit M, Williams K and Van Der Tol J 2019 Past, present and future of InP-based photonic integration *APL Photonics* **4** 050901
[58] Yi A, Wang C, Zhou L, Zhu Y, Zhang S, You T, Zhang J and Ou X 2022 Silicon carbide for integrated photonics *Appl. Phys. Rev.* **9** 031302
[59] Yi A *et al* 2020 Wafer-scale 4H-silicon carbide-on-insulator (4H–SiCOI) platform for nonlinear integrated optical devices *Opt. Mater.* **107** 109990
[60] Zheng Y, Pu M, Yi A, Ou X and Ou H 2019 4H-SiC microring resonators for nonlinear integrated photonics *Opt. Lett.* **44** 5784–7
[61] Zheng Y *et al* 2019 High-quality factor, high-confinement microring resonators in 4H-silicon carbide-on-insulator *Opt. Express* **27** 13053–60
[62] Wang C *et al* 2021 High-Q microresonators on 4H-silicon-carbide-on-insulator platform for nonlinear photonics *Light Sci. Appl.* **10** 139
[63] Lopez-Rodriguez B *et al* 2023 High-quality amorphous silicon carbide for hybrid photonic integration deposited at a low temperature *ACS Photonics* **10** 3748–54
[64] Lukin D M, Guidry M A and Vučković J 2020 Integrated quantum photonics with silicon carbide: challenges and prospects *PRX Quantum* **1** 020102
[65] Yang J, Guidry M A, Lukin D M, Yang K and Vučković J 2023 Inverse-designed silicon carbide quantum and nonlinear photonics *Light Sci. Appl.* **12** 201
[66] Lukin D M *et al* 2020 4H-silicon-carbide-on-insulator for integrated quantum and nonlinear photonics *Nat. Photon.* **14** 330–4
[67] Elshaari A W, Pernice W, Srinivasan K, Benson O and Zwiller V 2020 Hybrid integrated quantum photonic circuits *Nat. Photon.* **14** 285–98

[68] Kaur P, Boes A, Ren G, Nguyen T G, Roelkens G and Mitchell A 2021 Hybrid and heterogeneous photonic integration *APL Photonics* **6** 061102
[69] Puckett M W *et al* 2021 422 million intrinsic quality factor planar integrated all-waveguide resonator with sub-MHz linewidth *Nat. Commun.* **12** 934
[70] Corato-Zanarella M, Ji X, Mohanty A and Lipson M 2024 Absorption and scattering limits of silicon nitride integrated photonics in the visible spectrum *Opt. Express* **32** 5718–28